

N O T I C E

THIS DOCUMENT HAS BEEN REPRODUCED FROM
MICROFICHE. ALTHOUGH IT IS RECOGNIZED THAT
CERTAIN PORTIONS ARE ILLEGIBLE, IT IS BEING RELEASED
IN THE INTEREST OF MAKING AVAILABLE AS MUCH
INFORMATION AS POSSIBLE

(NASA-TM-81409) SUMMARY OF ADVANCED METHODS
FOR PREDICTING HIGH SPEED PROPELLER
PERFORMANCE (NASA) 14 p HC A02/MF A01

N80-15051

CSSL 01A

G3/02 Unclass
46641

NASA Technical Memorandum 81409

SUMMARY OF ADVANCED
METHODS FOR PREDICTING
HIGH SPEED PROPELLER
PERFORMANCE

L. A. Bober and G. A. Mitchell
Lewis Research Center
Cleveland, Ohio

Prepared for the
Eighteenth Aerospace Sciences Meeting
sponsored by the American Institute of Aeronautics and Astronautics
Pasadena, California, January 14-16, 1980

RECEIVED
NASA
AUG 15 1980

SUMMARY OF ADVANCED METHODS FOR PREDICTING HIGH SPEED PROPELLER PERFORMANCE

L. J. Bober* and G. A. Mitchell**
NASA-Lewis Research Center, Cleveland, Ohio

Abstract

Three advanced analyses for predicting aircraft propeller performance at high subsonic speeds are described. Two of these analyses use a lifting line representation for the propeller blades and vortex filaments for the blade wakes but differ in the details of the solution. The third analysis is a finite difference solution of the unsteady, three-dimensional Euler equations for the flow between adjacent blades. Analysis results are compared to data for a high speed propeller having 8 swept blades integrally designed with the spinner and nacelle. These analyses provide tools for the propeller designer ranging from a short running program for initial design studies to a very long running program for checking final configurations.

Symbols

C_p	power coefficient, power/
C_T	thrust coefficient, thrust/
D	propeller diameter
dC_p/dx	elemental power coefficient
J	advance ratio, V_∞ / nD
M_{tip}	relative (helical) Mach number at blade tip
M_∞	free stream Mach number
n	propeller rotational speed
V_∞	free stream velocity
x	radial location divided by propeller tip radius
$\beta_{3/4}$	blade angle at $x = 3/4$ relative to plane of rotation
η_{app}	propeller apparent efficiency
ρ_∞	free stream density

Introduction

The increased emphasis of fuel conservation in the world has stimulated a renewed interest in the turboprop as a viable propulsion system for high speed commercial aircraft. In the past it was known that propellers were highly efficient at cruise speeds up to approximately Mach 0.65 (fig. 1)¹. However, above this speed large compressibility losses on the propeller blading caused the efficiency to fall rapidly. Recent technology advances resulting from the Advanced Turboprop Program managed by NASA-Lewis Research Center have indicated that high speed turboprops can be designed with installed propulsive efficiencies at Mach 0.8

cruise that would be about 15 percent higher than the best advanced turbofan.

To achieve these goals the advanced turboprop must be capable of high efficiency at Mach 0.8 cruise above 9.144 Km (30,000 ft) altitude. At these conditions, the combination of cruise speed and blade rotational speed causes the local blade Mach number to vary from just over 0.8 at the blade hub to supersonic at the tip. Therefore, unique aerodynamic concepts are required to reduce blade compressibility losses and attain high efficiency (fig. 2). These include a proper shaping of the nacelle to reduce inboard blade Mach number, spinner area ruling to prevent inboard blade choking, blade sweep to reduce outboard blade local Mach number, and thinner blades to reduce drag rise Mach number. In addition, to hold propeller diameter to a reasonable value, a high power (or disk) loading and concomitantly a large number of blades (8 or 10) are required. The inboard portion of the propeller then operates as a cascade rather than isolated blades.

The above design concepts along with the attendant mixed subsonic and supersonic flows present a complicated analysis problem that is beyond the scope of traditional analysis tools based on the work of S. Goldstein². Goldstein's potential flow analysis is limited to lightly loaded propellers having straight blades. Compressibility effects and supersonic flow at the blade tips cannot be accounted for and the presence of a centerbody and its attendant flow fields is not recognized. The work of Theodorsen³ improved upon the analysis by removing the light loading restriction.

Strip analysis programs based upon these potential flow analyses have been modified in an attempt to account for some of the turboprop design concepts. For example, the simple cosine rule is used to account for blade sweep, the radial variation of axial velocity generated by the spinner/nacelle is accounted for, and a cascade correction is made to the airfoil characteristics in the inboard propeller region. More recent analyses are now emerging that are based on the equations of Biot-Savart.

*Aerospace Engineer, Member AIAA

**Aerospace Engineer

Strip analysis programs using these equations still use the modifications described above, but now include a swept lifting line capability and the ability to account for supersonic tip effects to some degree. Additional work on swept lifting line analyses and the development of more sophisticated lifting surface analyses are needed to more accurately predict propeller performance. Such analyses must define the blade and body geometry and evaluate the resulting complex flow fields in a more rigorous manner.

This paper will discuss two types of analyses, lifting line and lifting surface analyses. In a lifting line analysis each propeller blade is represented by a single line of vorticity and in a lifting surface analysis each blade is represented as a solid surface. Before considering the advanced analysis methods for predicting high speed propeller performance a discussion of the established approach to propeller performance analysis will be given. This will provide background information which will facilitate the understanding of the advanced methods. Two advanced lifting line analyses and one advanced lifting surface analysis being developed under the NASA Advanced Turboprop Program will be described. These advanced methods are still under development but some preliminary results from the lifting line analyses will be compared to data. The lifting surface analysis is not as far along in the development process as the lifting line analyses and only some qualitative results from this analysis will be presented.

Established Approach

This existing analysis is based on the work of Goldstein² and its salient features are indicated in figure 3. When the propeller blade is represented by a single line of vorticity (bound vortex) in a lifting line type of analyses, the nonuniform spanwise loading on the blade causes a continuous sheet of vorticity (vortex wake) to extend downstream to infinity. This continuous sheet of vorticity is shown in the sketch in figure 2 as a finite number of vortex filaments but it would more correctly be represented as an infinite number of vortex filaments. This vortex wake is important because it causes an induced velocity at the propeller which changes the local angle of attack of the propeller blade.

Due to the limited computing capability at the time, Goldstein used a simplified model so that he could obtain a closed form analytical solution for the induced flow at the propeller due to the wake. He assumed the vortex wake was composed of a rigid helical vortex sheet which corresponds to the optimum spanwise loading of a lightly loaded propeller³ just as a planar wake corresponds to an elliptically loaded wing⁴. The wake shown in figure 3 is a rigid helical vortex sheet. The intersection of this wake with a plane normal to the axis of rotation of the propeller is a straight line. In addition the pitch of a rigid heli. does not

change with axial location. Goldstein's results² were applicable only to single rotation propellers but Theodorsen⁵ determined the induced flow for optimally loaded coaxial counter-rotating propellers experimentally using an electrical analogy. In both of these studies the propeller was restricted to having straight blades and there was no provision for a nacelle since the vortex wake extends to the axis.

These wake effects are used in a strip analysis. In this procedure the conditions at each radial location on the propeller blade are determined as if the entire propeller was operating at the local inflow velocity. The total velocity of the air relative to the blade at a given radius is the vector sum of the flight velocity, the rotational velocity and the induced velocity which is obtained from Goldstein's or Theodorsen's results. Knowing the velocity and the blade geometry allows the local blade angle of attack to be determined and the blade lift and drag can be determined from two-dimensional airfoil data. Swept blades are taken into account through the use of the cosine rule⁴. These forces are resolved into thrust and torque components which are integrated radially to give the propeller thrust, torque, power and efficiency.

It is important to note that for any propeller operating condition the effect of the wake is assumed to be the same as for an optimally loaded propeller even if there are a nacelle and spinner present. The presence of the nacelle is taken into account in an approximate manner. The radially varying flow at the propeller is used instead of the free stream velocity when calculating the local blade angle of attack for each strip. This radially varying inflow is determined from a solution for the flow around the isolated nacelle (no propeller).

This established approach to propeller performance analysis is embodied in a computer program and serves as a basis for comparison for the advanced analysis methods.

Advanced Analysis Methods

Curved Lifting Line Analysis

An analysis which includes the nacelle effect on the wake in a simple manner and accounts for swept propeller blades has been developed by Sullivan⁶ under a grant from the NASA-Lewis Research Center and is summarized in figure 4. In this analysis the wake is represented by a finite number of helical vortex filaments instead of the continuous sheet of vorticity used by Goldstein and Theodorsen. Each filament has constant pitch but its location relative to the other filaments is arbitrary. At any radial location on the blade the induced flow due to each filament is calculated by using the Biot-Savart equation⁴ and the total induced velocity is obtained by summing over all the filaments. This analysis is currently restricted to single rotation propellers.

41
The blades are represented by curved lifting lines which can have any arbitrary shape although all the blades on a single propeller must have the same shape. The nacelle shape is restricted to an infinite circular cylinder since the wake rigid helical filaments cannot contract in the radial direction.

The strengths of the individual wake filaments are related to the spanwise variation of the bound vortex strength. Since both of these are unknown the blade and wake vortex strengths are solved simultaneously. This is done by placing the bound vortex along the quarter chord line and solving for the vortex strengths which cause the flow to be tangent to the blade mean camber line along the three-quarter chord line. The lift coefficient of the blade at any radial location is then determined from the bound vortex strength at the same radius thus obviating the need for any two-dimensional airfoil data.

Propeller Nacelle Interaction Analysis

Another advanced lifting line analysis⁶ was developed at United Technologies Research Center under contract to the NASA-Lewis Research Center. This analysis has more extensive capabilities which are summarized in figure 5. The wake is again represented by a finite number of vortex filaments which are placed along stream surfaces so that they conform to the shape of the nacelle. This wake model can be applied to both single and coaxial counter rotating propellers. The propeller can have blades of any arbitrary shape and the nacelle can be any axisymmetric geometry.

The first step in this analysis is the calculation of the inviscid flow around the nacelle only. The results from this calculation are used to locate the wake vortex filaments around the nacelle and to determine the inflow velocity at the propeller as a function of radial location. The induced velocity is determined by summing the induced flow from the individual filaments and the swept lifting line. The local blade angle of attack can then be determined and the lift and drag can be obtained from two-dimensional airfoil and cascade data. These forces are resolved into thrust and torque components so that the propeller performance can be calculated. A final optional step is to use the blade forces in a circumferentially averaged (axisymmetric) viscous compressible flow calculation. The results from this calculation are used to ensure the velocities between the blades and downstream of the propeller do not get high enough to result in large losses caused by shock waves. They are also used to determine the drag of the nacelle in the presence of the propeller.

A propeller operating at either high flight speed or high rotational speed can have portions of the blade moving at supersonic speeds relative to the undisturbed flow.

For these conditions additional effects must be considered (fig. 6). In a supersonic flow a disturbance is felt only in a conical region downstream of the disturbance (region of influence). Thus when the induced velocity due to the wake is calculated it is necessary to limit the region over which each wake filament has an effect. A second consideration is when the tip of the blade is supersonic the flow becomes highly three-dimensional near the tip due to the tip Mach cone. This is taken into account by applying a correction to the two-dimensional airfoil data.

Advanced Lifting Surface Analysis

A lifting surface analysis has been developed at the NASA-Ames Research Center by applying an existing three-dimensional flow solver to propeller geometries⁷. The first step in this analysis is to generate a grid which conforms to the shape of the nacelle as shown in figure 7. The side view of the grid shows the nacelle and propeller blades and the front view shows the grid between two adjacent blades of an 8 bladed propeller. The nacelle is required to be axisymmetric so that the flow between each two adjacent blades are the same and it is only necessary to solve for the flow between two blades. Beyond the tips and upstream and downstream of the blades the flow is assumed to be periodic. On all solid surfaces the flow is required to be tangent to the surface. The actual grid used in the calculations extends much further in the radial direction than is shown in figure 7.

The equations of motion in finite difference form are solved at discrete points in the grid. The equations used are the unsteady three-dimensional Euler equations which govern the inviscid flow of a compressible fluid and can accurately represent the total pressure variation caused by shock waves and the work done by the propeller. The equations are solved by marching in time using the implicit finite difference scheme of Beam and Warming⁸ until a steady state is reached. This analysis requires no wake modeling and no two-dimensional airfoil data.

An indication of the detailed flow predictions obtainable with this analysis is given in figure 8. Shown are the pressure distributions on both sides of a propeller blade at three spanwise locations. These results give the chordwise distribution of load on the blade, information that cannot be obtained from any of the other advanced analyses. Also indicated is a shock wave on the suction surface that extends across the entire span of the blade. These detailed three-dimensional results are important for improved aerodynamic, acoustic and structural performance. Current development efforts are being focused on improved boundary conditions on the blade surfaces.

Comparison With Data

24

The two advanced lifting line analyses and the Goldstein strip analysis (established approach) have been used to predict the performance of the SR1 propeller configuration⁹ shown in figure 9. This is a highly loaded propeller having eight blades with thirty degrees of sweep at the tip and designed for cruise at an altitude of 10.7 km (35,000 ft). At the design point the flight Mach number is 0.8 and the tip speed is 244 meters per second (800 fps) resulting in a tip relative Mach number of 1.15. As noted previously the advanced analyses are still under development and the following results should be considered preliminary.

Shown in figure 10 is a comparison of the predicted and measured power coefficient for the SR1 configuration at a free stream Mach number of 0.8. This propeller was designed to operate at a power coefficient of 1.7 at an advance ratio of 3.06. The analytical results were obtained for a blade angle, $\beta_{3/4}$, of 61.2°. Since the curved lifting line analysis can currently use only a uniform inflow velocity, this was taken to be equal to the free stream velocity. As noted previously the curved lifting line analysis assumes the blade drag is zero and this causes at least in part the under-prediction of power coefficient by this analysis. An estimate of the effect of nonuniform inflow shows about a one degree increase in blade angle of attack due to non-uniform inflow which would move the curved lifting line results into much better agreement with the 61.2° data since a one degree increase in blade angle of attack corresponds to a one degree increase in blade angle. Non-uniform inflow and a drag estimation procedure are planned for inclusion in this analysis in the near future.

The effect of the nacelle was taken into account in the established approach by using inflow velocities determined from an axisymmetric calculation of the isolated nacelle flow field using the method of reference 10. The established approach and the propeller nacelle interaction analysis both overpredict the power coefficient. The close agreement of the results from these two analyses does not mean that the many additional features included in the propeller nacelle interaction analysis have insignificant effects. A comparison of this analysis to the established approach for this configuration has shown that including wake distortion due to the nacelle causes an increase in predicted power coefficient; including supersonic tip effects causes a decrease in predicted power coefficient; and including region of influence considerations in the wake effect calculation causes an increase in predicted power coefficient. In the final results some effects have partially cancelled other effects. Refinements to the propeller nacelle interaction analysis are planned for the

initial inviscid calculation, the supersonic tip correction and the cascade correction to the isolated airfoil data.

The analytical results for apparent efficiency are compared to data in figure 11. The experimental results were obtained in the test program described in reference 9. The net efficiencies shown in ref. 9 are lower than the apparent efficiencies shown in fig. 11 because the net efficiency includes a penalty for the increased pressure drag on the nacelle due to the interaction of the propeller and nacelle flow field. Both the established approach and the propeller nacelle interaction analysis predict the peak efficiency to within about 1%. However, the results from both of these analyses seem to agree better with the 62.5° data than with the 61.2° data which is consistent with the predicted loading in figure 10. The curved lifting line analysis overpredicts the efficiency in part because of the zero drag assumption. The under-prediction of power by the curved lifting line analysis (fig. 10) also contributes to the over-prediction of efficiency. Efforts are continuing to understand and correct the over-prediction of efficiency by the curved lifting line analysis. In general the agreement between analysis and experiment is not as good for the efficiency as for the power coefficient. This results from the definition of efficiency, $\eta = J C_T / C_p$. An accurate prediction of efficiency thus requires accurate prediction of both power and thrust coefficient which is more difficult than the prediction of just the power.

The spanwise variation of loading predicted by the analyses is shown in figure 12. The difference in level is a direct result of different predictions of power coefficient by the analyses. The results of the Goldstein strip analysis and the curved lifting line analysis are similar in shape but the additional features included in the propeller nacelle interaction analysis cause a considerable change in the power loading distribution. This difference in shape of the curves is due to the inclusion of the high speed effects in the propeller nacelle interaction analysis. Since changing the spanwise loading distribution presents the greatest potential for improving propeller performance, inclusion of these effects becomes important for the design of high speed propellers with optimum performance.

Initial comparisons of the analytical results from these advanced methods with performance data have shown qualitative agreement and have identified areas requiring refinements. Detailed flow measurements are needed for verifying these analyses and making them available as analytical tools for designing improved propellers. An experimental program is planned for the NASA-Lewis Research

Center 8X6 foot wind tunnel to provide this detailed data. A laser velocimeter system (fig. 12) will be used to make these measurements since this type of system does not introduce any hardware which might disturb the flow.

Concluding Remarks

Three advanced analyses for predicting high speed propeller performance are being developed under the NASA Advanced Turboprop Program. The curved lifting line analysis is being modified to accept non-uniform inflow and to include blade drag. An improved inviscid calculation, a modified cascade correction to airfoil data and an improved supersonic tip correction are being included in the propeller nacelle interaction analysis. Initial comparisons of results from these two lifting line analyses with data show reasonable agreement. Initial results from the advanced lifting surface analysis show great potential for improving high speed propeller designs. Improved methods for treating boundary conditions on the blade surfaces are being implemented. After these analyses are verified through detailed comparisons with data, they will be available as analytical tools ranging from a short running program for initial design studies to a very long running program for checking final configurations.

References

1. Rohrbach, C., "A Report on the Aerodynamic Design and Wind Tunnel Test of a Prop-Fan Model", AIAA Paper 76-667, July, 1976.
2. Goldstein, S., "On the Vortex Theory of Screw Propellers", Royal Society (London) Proceedings, Vol. 123, No. 792, Apr. 6, 1929, pp. 440-465.
3. Theodorsen, T., Theory of Propellers, McGraw-Hill, New York, 1948.
4. Kueth, A. M., and Schetzer, J. D., Foundations of Aerodynamics, Wiley, New York, 1950.
5. Sullivan, J. P., "The Effect of Blade Sweep on Propeller Performance", AIAA Paper 77-716, June, 1977.
6. Egolf, T. A., Anderson, O. L., Edwards, D. E., and Landgrebe, A. J., "An Analysis for High Speed Propeller-Nacelle Aerodynamic Performance Prediction; Volume 1, Theory and Initial Application and Volume 2, User's Manual for the Computer Program", United Technologies Research Center, East Hartford, CT, R79-912949-19, June, 1979.
7. Chaussee, D. S., "Computation of Three-Dimensional Flow Through Prop Fans", Nielsen Engineering and Research, Inc., Mountain View, CA, NEAR-TR-199, June, 1979.
8. Beam, R. M., and Warming, R. F., "An Implicit Finite-Difference Algorithm for Hyperbolic Systems in Conservation-Law Form", Journal of Computational Physics, Vol. 22, No. 1, Sept., 1976, pp. 87-110.
9. Mikkelsen, D. C. and Blaha, B. J., Mitchell, G. A., and Wikete, J. E., "Design and Performance of Energy Efficient Propellers for Mach 0.8 Cruise", SAE Paper 770458, Mar. 1977; also NASA TM X-73612.
10. Chow, W. L., Bober, L. J., and Anderson, B. H., "Numerical Calculation of Transonic Boattail Flow", NASA TN D-7984, 1975.

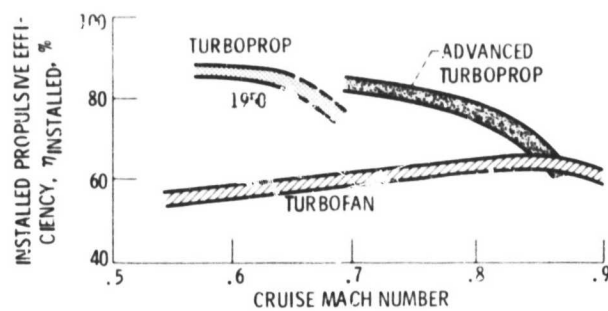


Figure 1. - Variation of installed cruise efficiency with Mach number.

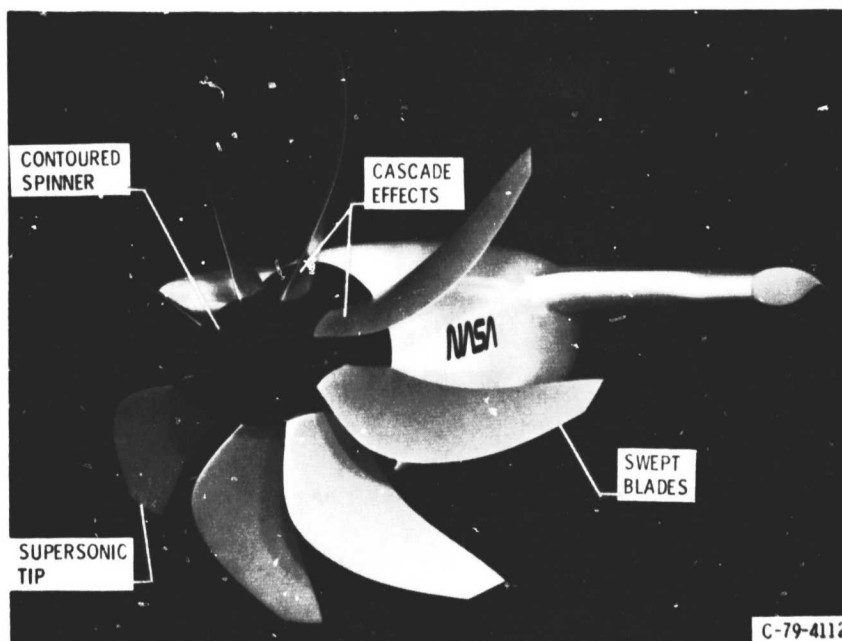


Figure 2. - Features of advanced high speed turboprop propulsion system which cause complex flow fields requiring advanced analyses.

ORIGINAL PAGE IS
OF POOR QUALITY

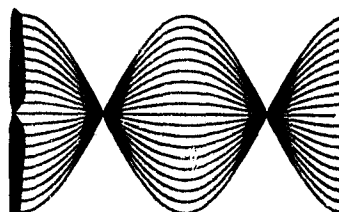
MODEL

WAKE - RIGID HELICAL VORTEX SHEET

SINGLE OR COUNTER ROTATION

BLADES - STRAIGHT LIFTING LINE

NACELLE - NONE



SOLUTION TECHNIQUE

STRIP ANALYSIS

CS-79-4089

Figure 3. - Summary of important features of an established approach to propeller performance analysis.

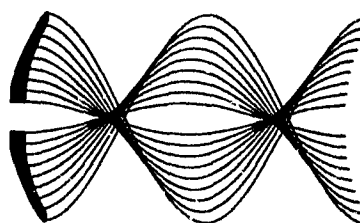
MODEL

WAKE - RIGID HELICAL VORTEX FILAMENTS

SINGLE ROTATION

BLADES - CURVED LIFTING LINE

NACELLE - INFINITE CYLINDER



SOLUTION TECHNIQUE

SIMULTANEOUS SOLUTION FOR BLADE

AND WAKE VORTEX STRENGTHS

CS-79-4088

Figure 4. - Summary of important features of the curved lifting line analysis.

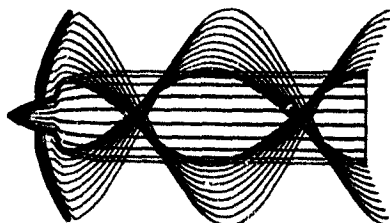
MODEL

WAKE - VORTEX FILAMENTS ALONG
STREAM SURFACES

SINGLE OR COUNTER
ROTATION

BLADES - CURVED LIFTING LINE

NACELLE - ARBITRARY GEOMETRY



SOLUTION TECHNIQUE

INVISCID NACELLE SOLUTION TO
LOCATE WAKE FILAMENTS

INDUCED ANGLE OF ATTACK DUE
TO WAKE

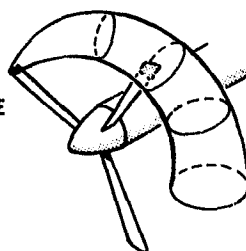
BLADE FORCES USED IN
CIRCUMFERENTIALLY AVERAGED
VISCIOUS FLOW

CS-79-4090

Figure 5. - Summary of important features of the propeller nacelle interaction analysis.

SUPERSONIC FLOW REGIONS OF INFLUENCE

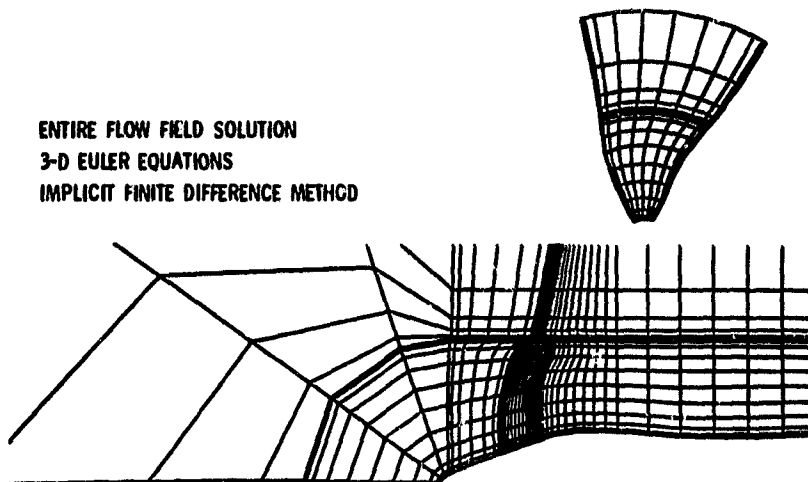
SUPERSONIC TIP CORRECTION



CS-79-3788

Figure 6. - High speed effects included in the propeller nacelle interaction analysis.

ENTIRE FLOW FIELD SOLUTION
3-D EULER EQUATIONS
IMPLICIT FINITE DIFFERENCE METHOD



CS-79-4124

Figure 7. - Summary of important features of the lifting surface analysis.

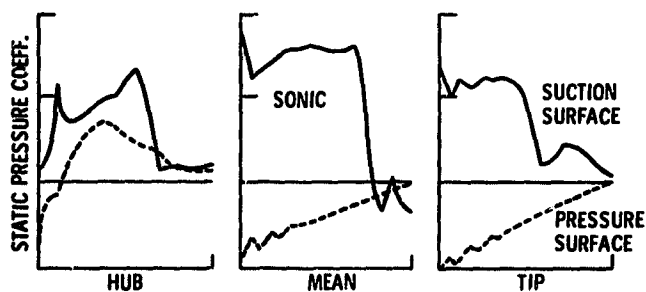
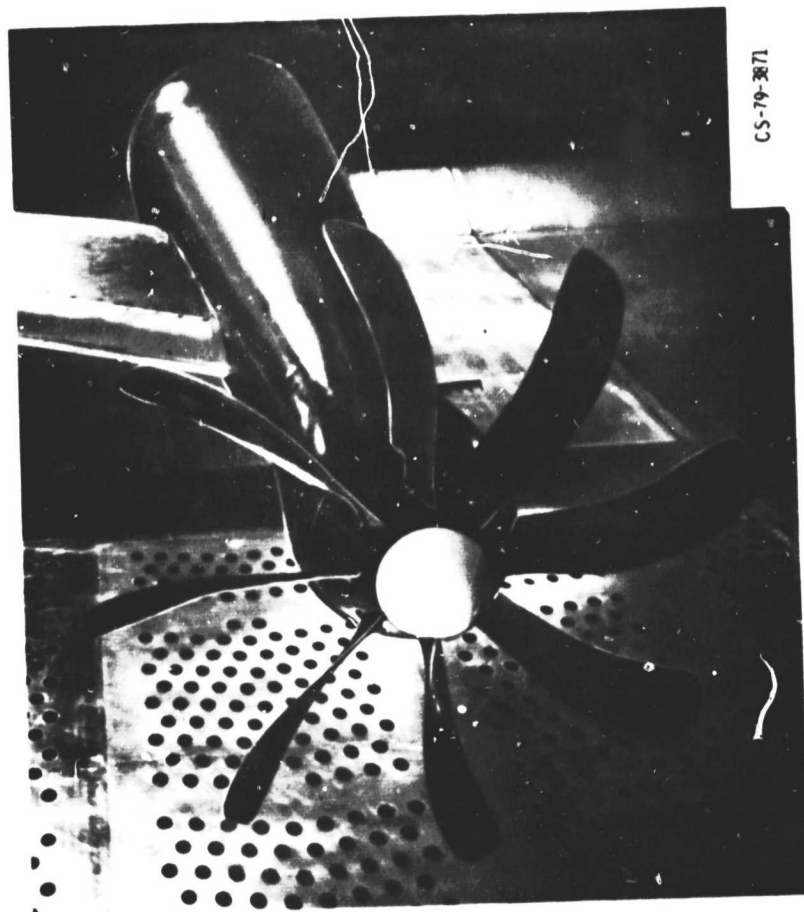


Figure 8. - Blade pressure distributions predicted by the advanced lifting surface analysis. 8 bladed propeller; $M_{\infty} = 0.8$; $M_{tip} = 1.15$.



CS-79-3871

Figure 9. - The SR1 propeller configuration in the NASA-Lewis Research Center 8- by 6-Foot Wind Tunnel.

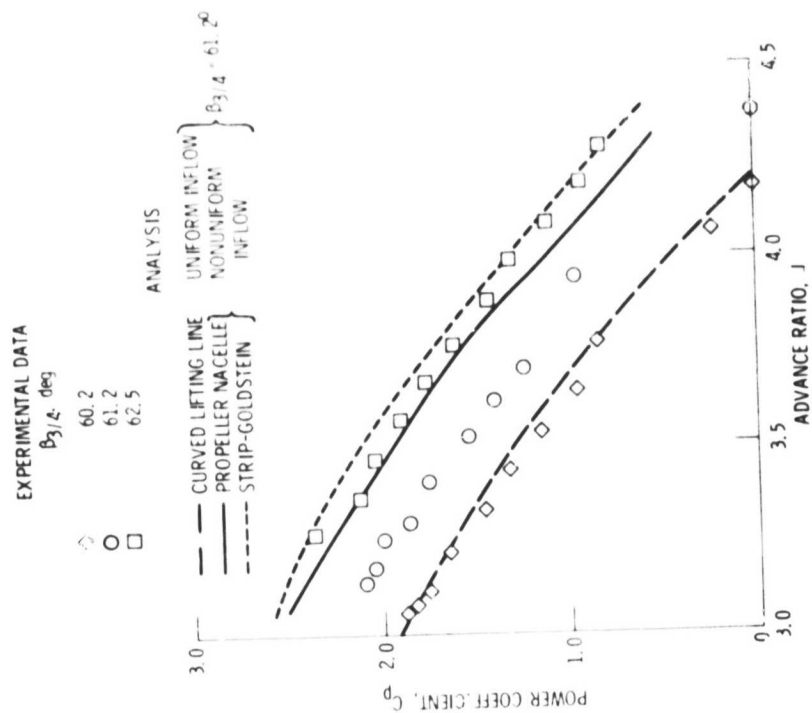


Figure 10. - Comparison of analytical and experimental power coefficient for SR1 propeller configuration. $M_\infty = 0.8$.

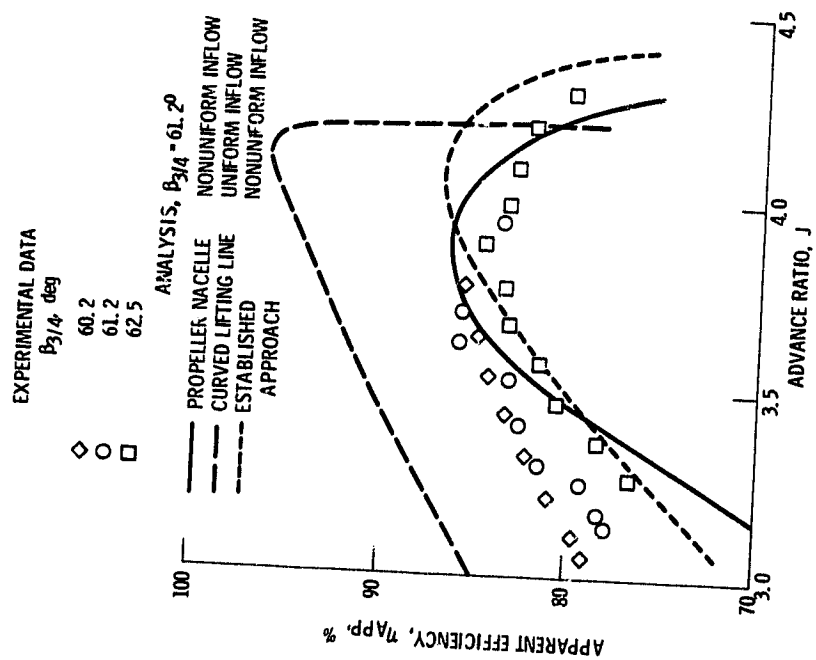


Figure 11. - Comparison of analytical and experimental efficiency for SRI propeller configuration. $M_\infty = 0.80$.

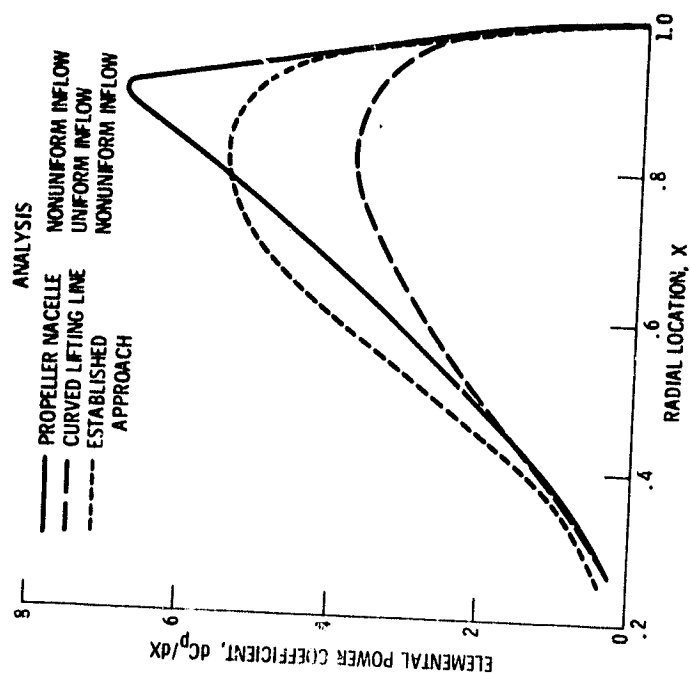


Figure 12. - Analytical results for elemental power coefficient for SRI propeller configuration. $M_\infty = 0.8$, $J = 3.06$, $\beta_{3/4} = 61.2^\circ$.

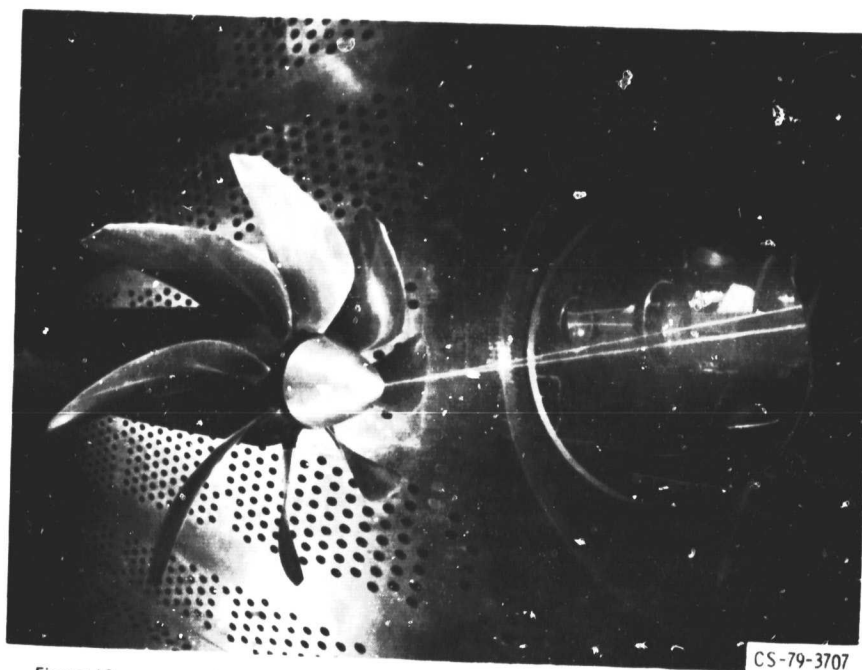


Figure 13. - Laser velocimeter in NASA-Lewis Research Center 8- by 6-Foot Wind Tunnel for making detailed flow measurements to be used in verifying advanced analyses.

ORIGINAL PAGE IS
OF POOR QUALITY